

This article was downloaded by:

On: 26 January 2011

Access details: *Access Details: Free Access*

Publisher *Taylor & Francis*

Informa Ltd Registered in England and Wales Registered Number: 1072954 Registered office: Mortimer House, 37-41 Mortimer Street, London W1T 3JH, UK



## Liquid Crystals

Publication details, including instructions for authors and subscription information:

<http://www.informaworld.com/smpp/title~content=t713926090>

### The effects of the bulkiness of terminal chains on the stability of smectics deduced from the crystal structures of isomeric chiral biphenyl esters

Shoko Kurogoshi; Kayako Hori

Online publication date: 06 August 2010

**To cite this Article** Kurogoshi, Shoko and Hori, Kayako(1997) 'The effects of the bulkiness of terminal chains on the stability of smectics deduced from the crystal structures of isomeric chiral biphenyl esters', *Liquid Crystals*, 23: 1, 127 – 136

**To link to this Article:** DOI: 10.1080/026782997208730

**URL:** <http://dx.doi.org/10.1080/026782997208730>

PLEASE SCROLL DOWN FOR ARTICLE

Full terms and conditions of use: <http://www.informaworld.com/terms-and-conditions-of-access.pdf>

This article may be used for research, teaching and private study purposes. Any substantial or systematic reproduction, re-distribution, re-selling, loan or sub-licensing, systematic supply or distribution in any form to anyone is expressly forbidden.

The publisher does not give any warranty express or implied or make any representation that the contents will be complete or accurate or up to date. The accuracy of any instructions, formulae and drug doses should be independently verified with primary sources. The publisher shall not be liable for any loss, actions, claims, proceedings, demand or costs or damages whatsoever or howsoever caused arising directly or indirectly in connection with or arising out of the use of this material.

# The effects of the bulkiness of terminal chains on the stability of smectics deduced from the crystal structures of isomeric chiral biphenyl esters

by SHOKO KUROGOSHI and KAYAKO HORI\*

Department of Chemistry, Ochanomizu University, Otsuka, Bunkyo-ku,  
Tokyo 112, Japan

(Received 7 January 1997; accepted 6 February 1997)

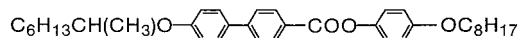
Single crystal X-ray analyses have been performed on 4-octyloxyphenyl 4'-[(S)-1-methylheptyloxy]biphenyl-4-carboxylate (8\*O-O8) and 4-[(S)-1-methylheptyloxy]phenyl 4'-octyloxybiphenyl-4-carboxylate (8O-O8\*), with the phase sequences Cr-SmC\*-Ch-I and Cr-SmX-SmC\*-SmA-I, respectively. Both crystals have smectic-like layer structures, in which the molecular tilt angles are 10° and 30°, respectively. In the crystal phase of 8\*O-O8, biphenyl moieties are twisted probably because of steric hindrance of the bulky chiral chains linked to them, whereas in 8O-O8\* they are nearly planar due to the conjugation between the alkoxy oxygen atoms and the carbonyl groups. From comparison of the properties with those of other related compounds, it is concluded that the conformation of the biphenyl moieties are closely related to the stability of smectic phases.

## 1. Introduction

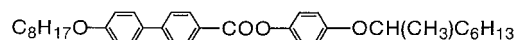
For the purpose of elucidating the factors controlling liquid crystalline behaviour, we have attempted to find the relationship of mesogenicity to molecular interactions in crystal structures. As a result of single crystal X-ray analyses of a series of chiral biphenyl esters with the identical core moiety  $-C_6H_4-C_6H_4-COO-C_6H_4-$ , it was found that they are classified into three groups in the properties of molecular structure, tilt angle in the crystalline state, and the liquid crystalline phase sequence [1]. In the first group, the biphenyl moiety is sandwiched by an alkoxy oxygen atom and a carbonyl group, which can conjugate through the biphenyl moiety. In the crystal phases, the alkoxy oxygen atoms and the carbonyl groups are closely faced between adjacent molecules, leading to large overlappings of biphenyl moieties, and hence to small tilt angles. Oxygen atoms in alkoxy groups seem to play an important role in the formation of layer structures, especially the SmA phase. In the second and third groups, the biphenyl moiety attaches an alkyl chain and the bulky 2-methylbutyl group, respectively, resulting in no conjugation as in the first group. In the second group, small tilt angles (large molecular overlappings in a smectic-like layer) are still observed, in accordance with the existence of the SmA phase. In the third group, large tilt angles are observed,

also related to the existence of a largely tilted SmC\* phase or no smectics.

In this work, to elucidate the effects of chiral groups and alkoxy oxygen atoms on crystal packing and mesomorphic behaviour, the following two biphenyl esters were studied. 4-Octyloxyphenyl 4'-[(S)-1-methylheptyloxy]biphenyl-4-carboxylate (abbreviated as 8\*O-O8)



4-[(S)-1-Methylheptyloxy]phenyl 4'-octyloxybiphenyl-4-carboxylate (8O-O8\*)



They have identical cores but the terminal *n*-alkyl and chiral chains are exchanged, to give the different phase sequences: Cr-SmC\*-Ch-I for 8\*O-O8 and Cr-SmX-SmC\*-SmA-I for 8O-O8\* [2].

This paper describes the crystal structures of 8\*O-O8 and 8O-O8\*, and discusses these in relation to the liquid crystalline behaviour in comparison with those of other chiral biphenyl esters.

## 2. Experimental

Both materials were donated by Chisso Petrochemical Corporation. Phase transition temperatures and enthalpies were measured using a Seiko DSC22C system. Using a Perkin-Elmer System 2000 equipped with an *i*-Series FT-IR microscope, FT-IR spectra were measured as a function of temperature controlled by a Mettler FP80.

\*Author for correspondence.

Powder X-ray diffraction patterns were obtained on a Rigaku RU200 diffractometer.

Single crystals were grown from an acetone–methanol solution for 8\*O-O8 and an ethyl acetate–ethanol solution for 8O-O8\*. Cell parameter measurements and reflection data collection were done on a Rigaku AFC-7R four-circle diffractometer with  $\text{CuK}_\alpha$  radiation ( $\lambda = 1.54184 \text{ \AA}$ ) at room temperature. The data were collected by  $2\theta$ - $\omega$  scan with scan rates of  $8^\circ \text{ min}^{-1}$  ( $2\theta$ ) for 8\*O-O8 and  $4^\circ \text{ min}^{-1}$  ( $2\theta$ ) for 8O-O8\* up to  $2\theta = 120^\circ$ . Three standard reflections were measured after every 150 reflections for monitoring the stability of the experimental conditions. No significant change was observed. Corrections were performed for Lorentz and polarization factors, but not for absorption and extinction. Experimental details and crystal data are summarized in table 1.

The structures were solved by applying the programs SIR-88 [3] for 8\*O-O8 and MULTAN-88 [4] for 8O-O8\* and refined by the full-matrix least squares method on  $F^2$  using SHELXL-93 [5]. All the benzene rings were constrained to have regular hexagonal geometry with the C–C distance of  $1.39 \text{ \AA}$  and refined as rigid groups. Several bonds in chains were also restrained. In the process of refinement for 8\*O-O8, terminal atoms with remarkably large temperature factors were disordered or the temper-

ature factors were fixed to be 0.3. For 8O-O8\*, since all the carbon atoms in the longer chain of the chiral group had very large temperature factors and small peaks were found around them, they were disordered. All the non-hydrogen atoms, except for the atoms which are disordered or have fixed temperature factors, were refined anisotropically. The positions of the hydrogen atoms attached to the anisotropically refined carbon atoms were calculated geometrically (C–H distances; 0.96 for primary, 0.97 for secondary, 0.98 for tertiary and 0.93  $\text{ \AA}$  for aromatic), and the H atoms were included in the intensity calculation but not refined. Final results of refinements are shown in table 1. The large  $R$  value of 8O-O8\* is attributed to the highly disordered chiral chain and the poor crystallinity. The latter is also responsible for the large ESDs of the lattice parameters. Scattering factors were taken from the International Tables for Crystallography [6]. Tables 2 and 3 give the final atomic coordinates for non-hydrogen atoms of 8\*O-O8 and 8O-O8\*, respectively.

### 3. Results and discussion

#### 3.1. Molecular conformations

Figure 1 shows the molecular structures with numbering schemes for both compounds. For 8\*O-O8, there are four crystallographically independent molecules (A,

Table 1. Crystal data and final results of refinements.

	8*O-O8	8O-O8*
Formula		$\text{C}_{35}\text{H}_{46}\text{O}_4$
Molecular weight		530.75
Crystal shape		plate
Crystal size/mm	$0.6 \times 0.5 \times 0.05$	$0.4 \times 0.4 \times 0.02$
L.s. for cell const. <sup>a</sup>	25 ( $40 < 2\theta < 52^\circ$ )	19 ( $40 < 2\theta < 54^\circ$ )
Crystal system	triclinic	monoclinic
Space group	$P1$	$P2_1$
$a/\text{\AA}$	11.704(3)	31.952(11)
$b/\text{\AA}$	34.571(10)	5.527(9)
$c/\text{\AA}$	8.051(2)	8.971(11)
$\alpha/^\circ$	95.15(2)	90
$\beta/^\circ$	92.67(2)	90.37(7)
$\gamma/^\circ$	97.89(2)	90
$V/\text{\AA}^3$	3208(2)	1584(3)
$Z$	4	2
$d_x/\text{g cm}^{-3}$	1.099	1.112
$\mu/\text{mm}^{-1}$	0.548	0.555
$F(0\ 0\ 0)$	1152	576
No. of unique reflections	9487	2625
No. of obsd. refl. ( $> 2\sigma(I)$ )	6569	1385
$R(F)(> 2\sigma(I))^b$	0.0962	0.1204
$wR(F^2)(> 2\sigma(I))^c$	0.3279	0.3630
$S$	1.067	1.034

<sup>a</sup> Number of reflections with the  $2\theta$  range in parentheses.

<sup>b</sup>  $R(F) = \frac{\sum \|F_o| - |F_c|\|}{\sum |F_o|}$  for observed reflections.

<sup>c</sup>  $wR(F^2) = [\sum w(F_o^2 - F_c^2)^2 / \sum w(F_o^2)^2]^{1/2}$  for observed reflections, where  $w = [\sigma^2(F_o^2) + (0.2020P)^2 + 1.43P]^{-1}$  for 8\*O-O8 and  $w = [\sigma^2(F_o^2) + (0.2998P)^2 + 0.78P]^{-1}$  for 8O-O8\*. ( $P = [F_o^2 + 2F_c^2]/3$ ).

Table 2. Atomic coordinates and equivalent isotropic displacement parameters of non-hydrogen atoms for 8\*O–O8.  $U(\text{eq})$  is defined as one third of the trace of the orthogonalized  $U_{ij}$  tensor.

Atom	$x$	$y$	$z$	$U(\text{eq})$
O(1A)	0.4801(6)	0.5349(2)	0.8831(8)	0.098(2)
O(2A)	0.5723(4)	0.2392(2)	0.5335(6)	0.075(1)
O(3A)	0.4062(6)	0.2377(2)	0.3803(9)	0.105(2)
O(4A)	0.5781(5)	0.0807(2)	0.3542(7)	0.089(2)
C(1A)	0.4805(4)	0.4975(1)	0.8198(6)	0.073(2)
C(2A)	0.5529(4)	0.4762(1)	0.9041(5)	0.071(2)
C(3A)	0.5567(4)	0.4371(1)	0.8492(5)	0.066(2)
C(4A)	0.4882(4)	0.4194(1)	0.7100(5)	0.073(2)
C(5A)	0.4158(4)	0.4408(1)	0.6257(5)	0.076(2)
C(6A)	0.4119(4)	0.4799(1)	0.6806(6)	0.081(2)
C(7A)	0.4887(4)	0.3760(1)	0.6510(6)	0.067(2)
C(8A)	0.5832(3)	0.3576(1)	0.6915(6)	0.071(2)
C(9A)	0.5839(3)	0.3184(1)	0.6352(6)	0.071(2)
C(10A)	0.4901(4)	0.2977(1)	0.5384(6)	0.069(2)
C(11A)	0.3955(3)	0.3161(1)	0.4980(6)	0.078(2)
C(12A)	0.3948(3)	0.3552(1)	0.5543(6)	0.075(2)
C(13A)	0.4827(7)	0.2561(2)	0.4770(10)	0.076(2)
C(14A)	0.5710(4)	0.1992(1)	0.4845(6)	0.068(2)
C(15A)	0.6497(4)	0.1883(1)	0.3714(6)	0.078(2)
C(16A)	0.6528(4)	0.1488(1)	0.3238(6)	0.079(2)
C(17A)	0.5772(4)	0.1203(1)	0.3894(6)	0.072(2)
C(18A)	0.4986(4)	0.1312(1)	0.5025(6)	0.079(2)
C(19A)	0.4955(4)	0.1707(1)	0.5501(6)	0.080(2)
C(20A)	0.3998(7)	0.5586(2)	0.8206(11)	0.093(3)
C(21A)	0.2788(8)	0.5452(3)	0.8642(15)	0.119(3)
C(22A)	0.4389(11)	0.5999(3)	0.8892(14)	0.122(4)
C(23A)	0.5521(11)	0.6185(4)	0.8337(19)	0.151(5)
C(24A)	0.5712(15)	0.6609(4)	0.908(2)	0.172(6)
C(25A)	0.6787(18)	0.6851(5)	0.865(3)	0.248(11)
C(26A)	0.684(3)	0.7274(6)	0.932(4)	0.330(17)
C(27A)	0.792(3)	0.7506(11)	0.882(6)	0.47(3)
C(30A)	0.6680(11)	0.0685(3)	0.2630(15)	0.119(3)
C(31A)	0.6767(14)	0.0263(3)	0.2920(17)	0.155(5)
C(32A)	0.5876(13)	−0.0020(3)	0.195(2)	0.161(5)
C(33A)	0.6108(18)	−0.0440(4)	0.187(2)	0.202(8)
C(34A)	0.534(2)	−0.0736(5)	0.073(3)	0.273(14)
C(35A)	0.560(2)	−0.1149(5)	0.049(3)	0.266(12)
C(36A)	0.470(2)	−0.1422(8)	−0.059(4)	0.300
C(37A)	0.529(3)	−0.1785(8)	−0.074(4)	0.300
O(1B)	0.2121(5)	0.5151(2)	0.4074(7)	0.090(2)
O(2B)	0.4218(7)	0.2431(2)	−0.1247(9)	0.113(2)
O(3B)	0.2636(4)	0.2185(2)	−0.0003(7)	0.079(1)
O(4B)	0.3502(6)	0.0687(2)	−0.1994(8)	0.103(2)
C(1B)	0.2155(4)	0.4776(1)	0.3289(6)	0.076(2)
C(2B)	0.2964(4)	0.4730(1)	0.2104(6)	0.072(2)
C(3B)	0.3102(4)	0.4357(1)	0.1423(5)	0.073(2)
C(4B)	0.2431(4)	0.4029(1)	0.1928(6)	0.072(2)
C(5B)	0.1621(4)	0.4075(1)	0.3113(6)	0.085(2)
C(6B)	0.1483(4)	0.4449(2)	0.3794(6)	0.085(2)
C(7B)	0.2632(4)	0.3620(1)	0.1220(6)	0.070(2)
C(8B)	0.3713(4)	0.3569(1)	0.0665(7)	0.079(2)
C(9B)	0.3942(3)	0.3196(2)	0.0118(7)	0.093(3)
C(10B)	0.3090(4)	0.2874(1)	0.0126(7)	0.074(2)
C(11B)	0.2009(4)	0.2925(1)	0.0681(7)	0.091(2)
C(12B)	0.1779(3)	0.3298(1)	0.1228(7)	0.092(2)
C(13B)	0.3383(7)	0.2480(2)	−0.0503(10)	0.081(2)
C(14B)	0.2878(4)	0.1807(1)	−0.0426(6)	0.073(2)
C(15B)	0.3821(4)	0.1666(1)	0.0298(6)	0.079(2)
C(16B)	0.4037(4)	0.1288(2)	−0.0188(6)	0.082(2)

Table 2. (continued).

Atom	<i>x</i>	<i>y</i>	<i>z</i>	<i>U</i> (eq)
C(17B)	0.3311(5)	0.1051(1)	-0.1399(6)	0.081(2)
C(18B)	0.2368(4)	0.1192(1)	-0.2123(6)	0.087(2)
C(19B)	0.2152(4)	0.1570(2)	-0.1637(6)	0.085(2)
C(20B)	0.1323(9)	0.5370(3)	0.3268(13)	0.108(3)
C(21B)	0.0087(9)	0.5209(4)	0.351(2)	0.164(6)
C(22B)	0.1591(11)	0.5791(3)	0.3980(15)	0.127(4)
C(23B)	0.2713(13)	0.6010(4)	0.3567(19)	0.167(6)
C(24B)	0.2912(17)	0.6434(4)	0.427(2)	0.180(7)
C(25B)	0.3897(17)	0.6706(5)	0.375(3)	0.219(8)
C(26B)	0.3988(18)	0.7133(5)	0.442(4)	0.258(13)
C(27B)	0.5248(19)	0.7281(11)	0.437(5)	0.232(14)
C(27B')	0.479(6)	0.7355(18)	0.331(9)	0.28(3)
C(30B)	0.4528(10)	0.0554(3)	-0.1537(13)	0.112(3)
C(31B)	0.4703(10)	0.0203(3)	-0.2674(14)	0.115(3)
C(32B)	0.3764(11)	-0.0144(3)	-0.2751(15)	0.132(4)
C(33B)	0.3959(14)	-0.0483(3)	-0.3950(17)	0.156(5)
C(34B)	0.3067(16)	-0.0840(4)	-0.390(2)	0.207(8)
C(35B)	0.3322(19)	-0.1178(6)	-0.506(3)	0.215(9)
C(36B)	0.251(2)	-0.1552(7)	-0.504(4)	0.303(14)
C(37B)	0.288(3)	-0.1873(8)	-0.619(4)	0.300
O(1C)	0.0956(6)	0.0520(2)	0.2521(10)	0.117(2)
O(2C)	0.0301(4)	0.3486(2)	0.6376(6)	0.077(1)
O(3C)	-0.1238(7)	0.3234(2)	0.7665(11)	0.129(3)
O(4C)	-0.0478(5)	0.4984(2)	0.8534(7)	0.087(1)
C(1C)	0.0865(6)	0.0899(1)	0.3177(8)	0.097(3)
C(2C)	-0.0058(5)	0.0952(1)	0.4158(9)	0.126(4)
C(3C)	-0.0208(4)	0.1326(2)	0.4807(8)	0.105(3)
C(4C)	0.0566(5)	0.1649(1)	0.4475(7)	0.073(2)
C(5C)	0.1489(5)	0.1596(1)	0.3494(8)	0.092(2)
C(6C)	0.1639(5)	0.1222(2)	0.2845(7)	0.102(3)
C(7C)	0.0337(4)	0.2055(1)	0.5113(7)	0.070(2)
C(8C)	-0.0726(4)	0.2101(1)	0.5746(8)	0.105(3)
C(9C)	-0.0954(4)	0.2472(2)	0.6329(8)	0.104(3)
C(10C)	-0.0118(5)	0.2797(1)	0.6277(7)	0.079(2)
C(11C)	0.0945(4)	0.2752(1)	0.5644(9)	0.108(3)
C(12C)	0.1173(4)	0.2381(2)	0.5062(8)	0.114(4)
C(13C)	-0.0430(8)	0.3181(3)	0.6832(10)	0.085(2)
C(14C)	0.0063(4)	0.3858(1)	0.6881(6)	0.075(2)
C(15C)	-0.0873(4)	0.4006(1)	0.6175(6)	0.085(2)
C(16C)	-0.1074(4)	0.4384(2)	0.6690(6)	0.082(2)
C(17C)	-0.0339(4)	0.4614(1)	0.7910(6)	0.075(2)
C(18C)	0.0597(4)	0.4466(1)	0.8616(6)	0.083(2)
C(19C)	0.0798(4)	0.4088(1)	0.8101(6)	0.075(2)
C(20C)	0.2062(13)	0.0411(3)	0.2086(14)	0.133(4)
C(21C)	0.2780(14)	0.0413(5)	0.368(2)	0.200(8)
C(22C)	0.183(2)	0.0024(3)	0.1067(18)	0.226(11)
C(23C)	0.1266(15)	-0.0325(4)	0.1853(19)	0.175(6)
C(24C)	0.119(2)	-0.0671(4)	0.054(2)	0.256(12)
C(25C)	0.043(2)	-0.1038(5)	0.085(4)	0.345(19)
C(26C)	0.038(3)	-0.1431(6)	-0.012(4)	0.329(16)
C(27C)	0.097(3)	-0.1495(11)	-0.170(4)	0.277(14)
C(27C')	-0.025(6)	-0.1776(16)	0.062(8)	0.25(3)
C(30C)	-0.1487(8)	0.5136(3)	0.7992(13)	0.104(3)
C(31C)	-0.1404(10)	0.5537(3)	0.8928(16)	0.133(4)
C(32C)	-0.0408(12)	0.5826(3)	0.8498(18)	0.147(4)
C(33C)	-0.0210(15)	0.6234(4)	0.9244(19)	0.166(6)
C(34C)	0.0864(16)	0.6494(6)	0.887(3)	0.192(7)
C(35C)	0.113(3)	0.6912(7)	0.962(4)	0.257(15)
C(36C)	0.224(3)	0.7104(7)	0.900(5)	0.37(2)
C(37C)	0.201(3)	0.7522(8)	0.908(4)	0.300
O(1D)	-0.1807(8)	0.0326(2)	-0.2602(13)	0.150(3)

Table 2. (continued).

Atom	<i>x</i>	<i>y</i>	<i>z</i>	<i>U</i> (eq)
O(2D)	−0.2738(4)	0.3293(2)	0.1080(6)	0.078(1)
O(3D)	−0.1083(6)	0.3299(2)	0.2624(8)	0.107(2)
O(4D)	−0.2821(5)	0.4858(2)	0.2890(7)	0.089(2)
C(1D)	−0.1763(6)	0.0715(1)	−0.1916(8)	0.099(3)
C(2D)	−0.2574(5)	0.0920(2)	−0.2622(7)	0.097(3)
C(3D)	−0.2608(5)	0.1310(1)	−0.2047(6)	0.087(2)
C(4D)	−0.1832(5)	0.1494(1)	−0.0766(6)	0.067(2)
C(5D)	−0.1021(5)	0.1289(2)	−0.0060(7)	0.110(3)
C(6D)	−0.0986(6)	0.0900(2)	−0.0635(9)	0.128(4)
C(7D)	−0.1886(4)	0.1921(1)	−0.0117(6)	0.067(2)
C(8D)	−0.2822(3)	0.2107(1)	−0.0545(6)	0.079(2)
C(9D)	−0.2833(3)	0.2498(1)	0.0033(6)	0.075(2)
C(10D)	−0.1908(4)	0.2702(1)	0.1040(6)	0.073(2)
C(11D)	−0.0972(4)	0.2516(1)	0.1468(6)	0.082(2)
C(12D)	−0.0961(3)	0.2125(1)	0.0890(6)	0.078(2)
C(13D)	−0.1859(7)	0.3118(2)	0.1677(9)	0.076(2)
C(14D)	−0.2721(4)	0.3682(1)	0.1601(6)	0.070(2)
C(15D)	−0.3541(4)	0.3788(1)	0.2684(6)	0.079(2)
C(16D)	−0.3596(4)	0.4182(1)	0.3146(6)	0.077(2)
C(17D)	−0.2830(4)	0.4470(1)	0.2525(6)	0.076(2)
C(18D)	−0.2010(4)	0.4365(1)	0.1442(6)	0.075(2)
C(19D)	−0.1955(4)	0.3971(1)	0.0980(5)	0.073(2)
C(20D)	−0.0944(19)	0.0124(4)	−0.243(2)	0.229(10)
C(21D)	−0.133(2)	−0.0037(6)	−0.083(2)	0.242(9)
C(22D)	−0.095(2)	−0.0201(6)	−0.378(2)	0.308(18)
C(23D)	−0.182(3)	−0.0547(9)	−0.356(4)	0.46(3)
C(24D)	−0.144(3)	−0.0824(7)	−0.491(4)	0.52(3)
C(25D)	−0.218(3)	−0.1184(8)	−0.446(4)	0.44(3)
C(26D)	−0.201(3)	−0.1487(12)	−0.585(5)	0.47(3)
C(27D)	−0.283(5)	−0.1836(13)	−0.549(6)	0.50(4)
C(30D)	−0.3737(8)	0.4991(3)	0.3832(14)	0.110(3)
C(31D)	−0.3742(13)	0.5423(4)	0.363(3)	0.222(11)
C(32D)	−0.2714(16)	0.5718(5)	0.407(2)	0.38(3)
C(33D)	−0.3074(19)	0.6088(4)	0.352(2)	0.193(9)
C(34D)	−0.1904(18)	0.6315(5)	0.405(3)	0.221(11)
C(35D)	−0.175(2)	0.6746(5)	0.388(3)	0.208(8)
C(36D)	−0.056(3)	0.6941(9)	0.445(4)	0.38(2)
C(37D)	−0.036(3)	0.7355(9)	0.401(4)	0.371(19)

Occupancies for 27(B) and 27(C), 0.6; 27(B') and 27(C'), 0.4.

B, C and D). The biphenyl moieties of all the molecules are twisted, with the dihedral angles of 22.2(4)° (A), 25.5(4)° (B), 13.2(5)° (C) and 13.7(5)° (D). The chiral chains have almost all-*trans* conformations except for the terminal disordered atoms in molecules B and C, while in the normal chains the O4–C30–C31–C32 moieties have *gauche* conformations, with the torsion angles of 77.9(15)° (A), −58.2(14)° (B), 64.9(13)° (C) and −57(2)° (D).

In 8O-O8\*, on the other hand, the dihedral angle of the biphenyl moiety is 3.1(8)°, being nearly planar. The normal chain has an almost all-*trans* conformation, whereas the chiral chain is twisted and largely disordered.

### 3.2. Crystal packing

Figures 2 and 3 represent the crystal structures viewed along the *c* axis for 8\*O-O8 and the *b* axis for 8O-O8\*, respectively. Both crystals have smectic-like layer structures. In the crystal of 8\*O-O8, the large overlapping as a whole leads to the small tilt angle (10°) of the molecular long axis in a layer. Cores and chains among laterally neighbouring molecules are separately overlapped as a whole. Parallel pairs are formed between the molecules A and B and also C and D, in which ester linkages are closely arranged each other; the distances between O3A–O2B and O3D–O2C are approximately 3.4 Å and 3.3 Å, respectively. These pairs are further arranged in an antiparallel way.

Table 3. Atomic coordinates and equivalent isotropic displacement parameters of non-hydrogen atoms for 8O–O8\*.  $U(\text{eq})$  is defined as one third of the trace of the orthogonalized  $U_{ij}$  tensor.

Atom	$x$	$y$	$z$	$U(\text{eq})$
O(1)	0.6254(3)	0.449(2)	0.236(9)	0.107(3)
O(2)	0.3442(3)	0.373(2)	0.6392(10)	0.110(3)
O(3)	0.3269(3)	0.699(3)	0.5082(9)	0.128(4)
O(4)	0.1858(4)	0.375(3)	0.8921(14)	0.147(5)
C(1)	0.5865(2)	0.467(2)	0.0855(9)	0.093(4)
C(2)	0.5587(3)	0.6554(19)	0.0589(8)	0.100(4)
C(3)	0.5204(3)	0.661(2)	0.1316(9)	0.106(4)
C(4)	0.5100(2)	0.478(2)	0.2310(9)	0.092(4)
C(5)	0.5379(3)	0.290(2)	0.2577(9)	0.105(4)
C(6)	0.5761(3)	0.284(2)	0.1850(10)	0.118(5)
C(7)	0.4681(2)	0.485(2)	0.3094(9)	0.087(4)
C(8)	0.4406(3)	0.674(2)	0.2792(9)	0.111(5)
C(9)	0.4028(3)	0.689(2)	0.3548(10)	0.124(5)
C(10)	0.3926(3)	0.516(2)	0.4606(10)	0.094(4)
C(11)	0.4201(3)	0.327(2)	0.4908(9)	0.108(4)
C(12)	0.4578(3)	0.311(2)	0.4152(9)	0.099(4)
C(13)	0.3518(3)	0.541(3)	0.5403(12)	0.093(4)
C(14)	0.3041(3)	0.366(2)	0.7068(11)	0.117(5)
C(15)	0.2920(3)	0.548(2)	0.8043(11)	0.118(5)
C(16)	0.2524(4)	0.543(2)	0.8674(10)	0.111(4)
C(17)	0.2249(3)	0.356(3)	0.8330(12)	0.126(5)
C(18)	0.2370(4)	0.174(2)	0.7355(12)	0.120(5)
C(19)	0.2766(4)	0.179(2)	0.6724(10)	0.121(5)
C(20)	0.6395(4)	0.629(3)	−0.0692(13)	0.109(5)
C(21)	0.6844(4)	0.591(3)	−0.1137(14)	0.118(5)
C(22)	0.7018(5)	0.790(3)	−0.2114(17)	0.131(6)
C(23)	0.7472(5)	0.770(3)	−0.2474(16)	0.131(6)
C(24)	0.7653(5)	0.983(3)	−0.3286(18)	0.138(6)
C(25)	0.8119(5)	0.990(5)	−0.349(2)	0.184(11)
C(26)	0.8241(9)	1.203(5)	−0.442(3)	0.27(2)
C(27)	0.8701(9)	1.17(1)	−0.461(4)	0.33(3)
C(30)	0.1550(5)	0.209(4)	0.871(3)	0.203(13)
C(31)	0.1629(9)	0.019(5)	0.989(4)	0.244(16)
C(32)	0.1183(10)	0.380(6)	0.861(5)	0.132(11)
C(32')	0.1129(8)	0.268(9)	0.94(4)	0.142(13)
C(33)	0.099(3)	0.60(1)	0.79(1)	0.40(7)
C(33')	0.0914(19)	0.31(1)	0.79(5)	0.22(2)
C(34)	0.053(3)	0.54(3)	0.79(1)	0.34(7)
C(34')	0.057(4)	0.30(3)	0.91(2)	0.5(1)
C(35)	0.006(3)	0.50(5)	0.72(4)	0.3(2)
C(35')	0.038(2)	0.49(2)	0.81(9)	0.24(3)
C(36)	−0.041(3)	0.54(2)	0.78(1)	0.30(5)
C(36')	0.000(3)	0.44(3)	0.72(2)	0.4(1)
C(37)	−0.038(3)	0.70(2)	0.64(1)	0.31(5)
C(37')	−0.023(3)	0.67(2)	0.75(1)	0.27(3)

Occupancies for all the disordered atoms were fixed to be 0.5.

On the other hand, in the crystal of 8O–O8\*, the molecular long axis is tilted by 30° in a layer. Among adjacent molecules the planar biphenyl moieties largely overlap each other, and the two polar groups, ester and ether linkages, lie closely to form an antiparallel arrangement of molecules. The disordered chiral chains are interdigitated in the interface of the layers.

In order to estimate the packing efficiencies of each

section in the crystal structures, calculations using the program OPEC [7] were carried out for the atomic coordinates determined in this work [8]. As already mentioned, in the crystal of 8\*O–O8, core moieties and chains are segregated in a layer. Packing fractions are distinctly different between the two regions, 72 per cent for the cores and 58 per cent for the chains, as shown in figure 2. On the other hand, a smectic-like layer in

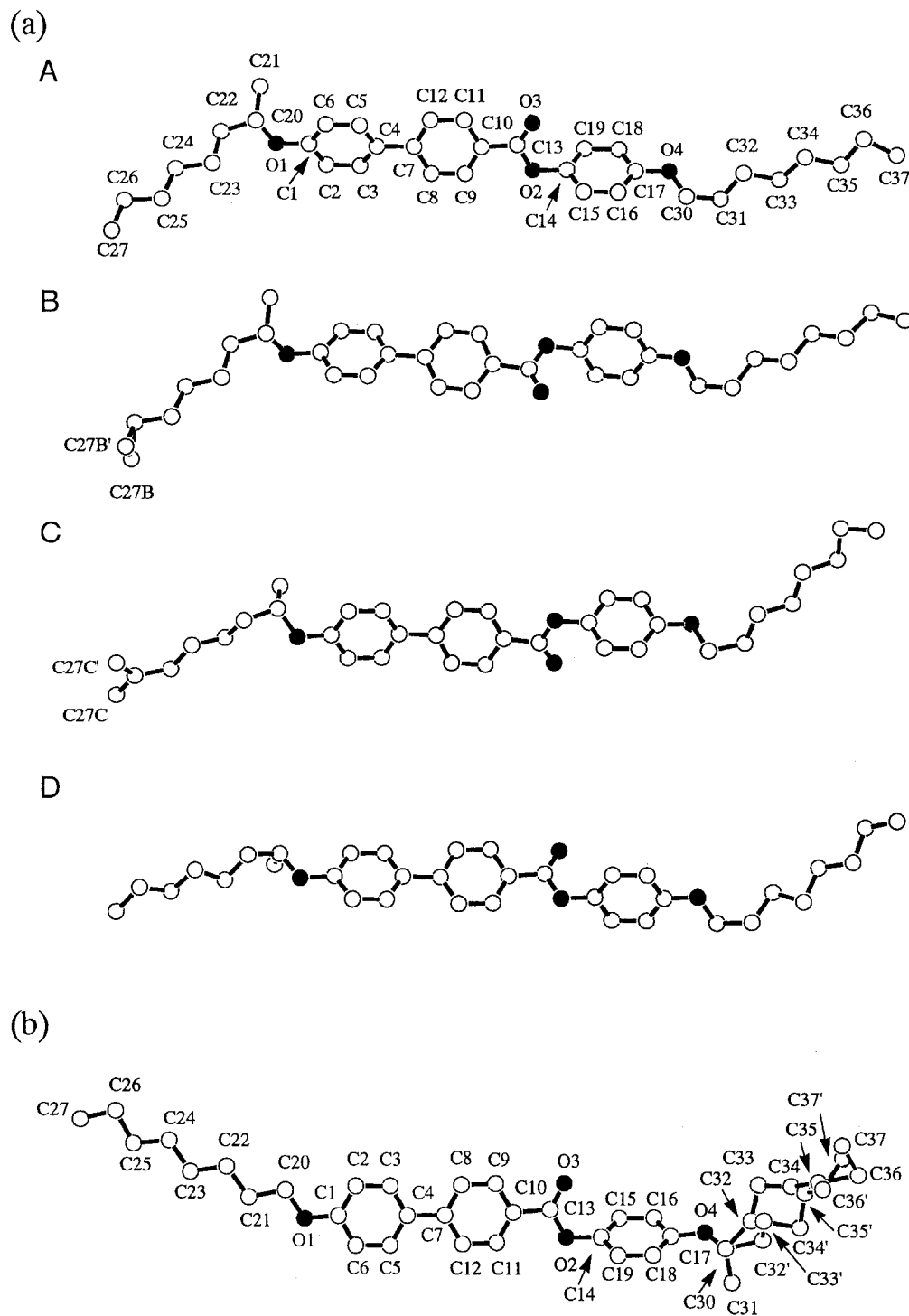


Figure 1. Molecular structures with numbering schemes of non-hydrogen atoms for (a) 8\*O-O8 and (b) 8O-O8\*. Filled circles denote oxygen atoms.

the crystal of 8O-O8\* is further divided into three regions, a layer composed of biphenyl moieties, a layer composed of single benzene rings and normal chains, and a layer composed of chiral chains. Packing fractions

are calculated to be 73, 60 and 51 per cent, respectively, as shown in figure 3. Therefore, it is suggested that for 8O-O8\* the overlap of planar biphenyl moieties in a layer have a significant effect on the crystal packing.



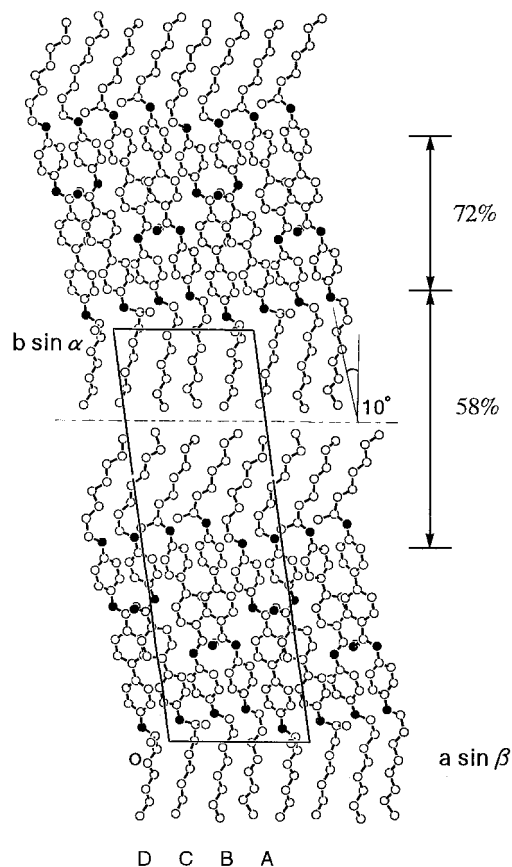


Figure 2. The crystal structure of 8\*O-O8 viewed along the  $c$  axis. Filled circles denote oxygen atoms. For molecules B and C, only one of the disordered atoms is shown for clarity. The numerical values beside the figure show the packing efficiencies calculated by the program OPEC.

### 3.3. Crystalline polymorphs of 8\*O-O8

Reflecting a subtle balance of intermolecular interactions, mesogenic compounds sometimes produce crystalline polymorphs. Thus, it is interesting to confirm the thermodynamic status of the crystal structures concerned.

Figure 4 shows DSC traces on heating for a powder specimen as supplied and plate crystals obtained from an acetone-methanol solution for 8\*O-O8. In the powder sample, there was a broad peak at 60°C attributed to a solid-solid phase transition, while the plate crystal showed no anomaly until it melted at 75.5°C. In order to examine the relationships between the two solid states, FT-IR spectral changes with increase of temperature were observed for KBr disks of both a powder sample and plate crystals. The change in wave number in the typical C=PdO stretching vibration region are shown in figure 5. The powder sample and the plate crystals gave quite different behaviour in the lower temperature less than about 60°C (dashed line), but they

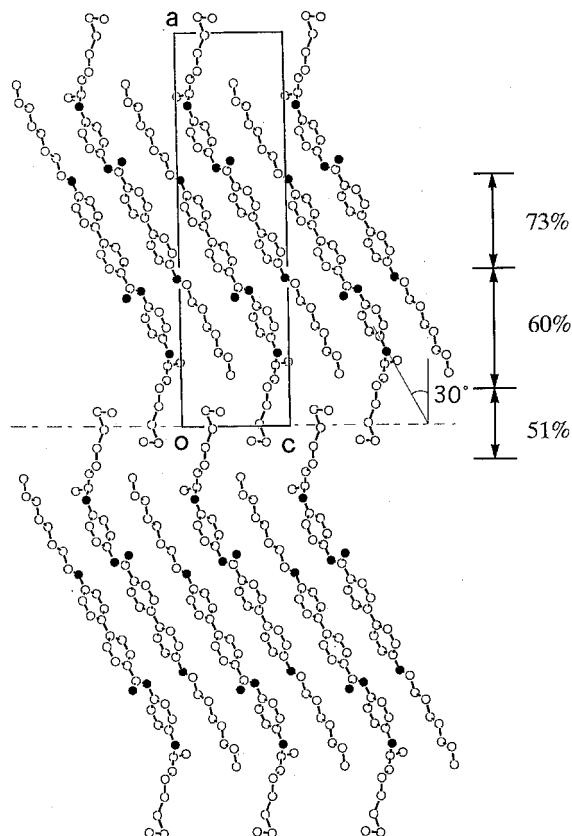


Figure 3. The crystal structure of 8O-O8\* viewed along the  $b$  axis. Filled circles denote oxygen atoms. Only one of the disordered chains is shown for clarity. The numerical values beside the figure show the packing efficiencies calculated by the program OPEC.

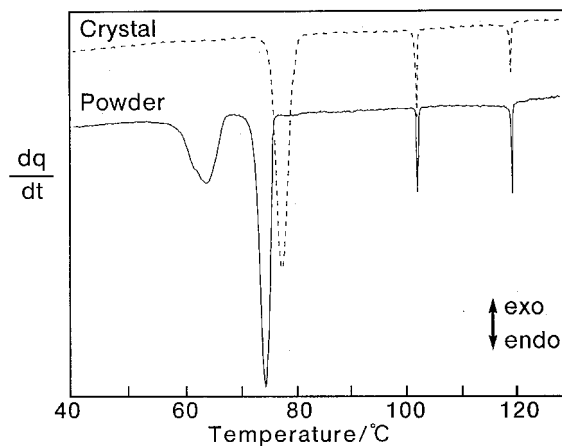


Figure 4. DSC traces on heating obtained for 8\*O-O8. Solid and dashed lines indicate the traces for the powder sample and the plate crystal, respectively.

followed similar paths into the isotropic state. Therefore, the plate crystal, the structure of which has been determined in this work is identified as the higher temperature

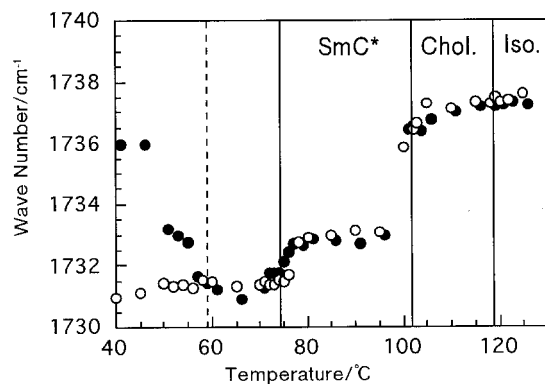


Figure 5. IR spectral changes in the C=O stretching vibration region on heating observed for 8\*O-8. Filled and open circles denote the values measured for the powder sample and the plate crystal, respectively.

phase, which exists as a supercooled state at room temperature. Furthermore, figure 6 shows the X-ray diffraction pattern measured for the powder sample and the simulated model for the plate crystal based on the crystal structure. Both solid states give obviously distinct patterns, with different layer spacings; 38.4 Å in the powder sample and 34.1 Å in the plate crystal. For 8O-8\*, no polymorphism in the solid state has been found.

#### 3.4. Comparison with related biphenyl esters

The crystal structures of 8\*O-8 and 8O-8\* are compared with those of other chiral biphenyl esters, particularly the following three compounds in which biphenyl moieties are sandwiched by alkoxy oxygen atoms and carbonyl groups:

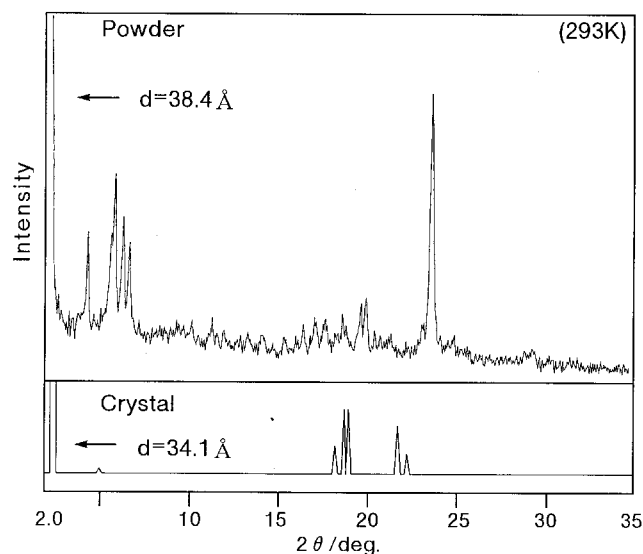
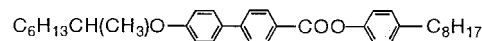
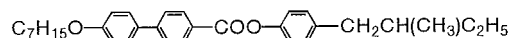


Figure 6. Powder X-ray diffraction pattern (upper) and simulated pattern for the plate single crystal (lower) of 8\*O-8.

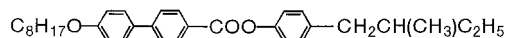
4-Octylphenyl 4'-[(S)-1-methylheptyloxy]biphenyl-4-carboxylate (8\*O-8)



4-[(S)-2-Methylbutyl]phenyl 4'-heptyloxybiphenyl-4-carboxylate (7O-5\*)



4-[(S)-2-Methylbutyl]phenyl 4'-octyloxybiphenyl-4-carboxylate (8O-5\*)



They show the identical phase sequence, Cr-SmC\*-SmA-Ch-I, in spite of their different terminal chains. The tilt angles in the crystal states were reported to be 10° for 8\*O-8 [8]†, 30° for 7O-5\* [9] and 8O-5\* [9]. The biphenyl moieties of 8\*O-8 are twisted by 21.4°, whereas those of 7O-5\* and 8O-5\* are nearly planar. Thus, similarities are found in 8\*O-8 and 8\*O-8, and in 8O-8\*, 7O-5\* and 8O-5\*. For 8\*O-8 and 8\*O-8, which have the same chiral chain directly linked to the biphenyl moiety, it is considered that the steric hindrance due to the chiral group twists the biphenyl moiety. On the other hand, for the three compounds, 8O-8\*, 7O-5\* and 8O-5\*, in which the normal alkoxy chains directly join to the biphenyl moieties, the biphenyl moieties adopt a planar structure by the conjugation between the alkoxy oxygen atoms and the carbonyl groups.

Taking these characteristics into account, it is concluded that what is substituted to the biphenyl moiety plays a significant factor in controlling the crystal packing and mesophase behaviour, as shown in figure 7. When the bulkiness of the chiral groups twists the biphenyl moieties, the instability of the smectic-like layer structures cause a narrowing of the temperature ranges

	50	100	150	(°C)	
8*O-8	Cr	SmC*	Chol.	I	
8*O-8	Cr	SmC*	SmA	Ch	I
8O-8*	Cr	SmX	SmC*	SmA	I
7O-5*	Cr	SmC*	SmA	Ch	I
8O-5*	Cr	SmC*	SmA	Ch	I

Figure 7. The temperature ranges of the mesophases for the chiral biphenyl esters.

† For disordered conformers, one of each pair was included in calculation with geometrically calculated hydrogen atoms.

of the smectic phases to about 28°C. On the other hand, when conjugation is possible due to the absence of the bulky chiral group near the biphenyl moiety, the layer structures are stabilized, inducing a wider temperature range of the smectic phases (81°C for 8O-O8\*, 82°C for 7O-5\* and 95°C for 8O-5\*).

#### 4. Conclusions

As a result of the crystal structure analyses for 8\*O-O8 and 8O-O8\*, and comparison with related biphenyl esters, we conclude that the molecules with the biphenyl moieties sandwiched by an alkoxy oxygen atom and a carbonyl group are divided into two subgroups. The position of the chiral group with respect to the core moiety determines whether the conjugation through the biphenyl moiety is possible or not. The existence of the chiral group near the biphenyl moiety probably depresses the stability of smectic phases as observed in 8\*O-O8 and 8\*O-8. Conversely, the conjugation seems to stabilize smectic phases as in 8O-O8\*, 7O-5\* and 8O-5\*.

The authors express their thanks to Chisso

Petrochemical Corporation for donating the samples and to Dr Yoichi Takanishi of the Tokyo Institute of Technology for help in the powder X-ray diffraction measurements.

#### References

- [1] ITO, K., and HORI, K., 1995, *Bull. Chem. Soc. Jpn.*, **68**, 3347.
- [2] INUKAI, T., SAITOH, S., INOUE, H., MIYAZAWA, K., TERASHIMA, K., and FURUKAWA, K., 1986, *Mol. Cryst. liq. Cryst.*, **141**, 251.
- [3] BURLA, M., C., CAMALL, M., CASCARANO, G., GIACOVAZZO, C., POLIDORI, G., SPAGNA, R., and VITERBO, D., 1989, SIR88, structure analysis programs, *J. appl. Cryst.*, **22**, 389.
- [4] DEBAEDEMAEKER, T., TATE, C., and WOOLFSON, M. M., 1985, MULTAN88, *Acta Cryst.*, **A41**, 286.
- [5] SHELDRIK, G. M., 1993, SHELXL93, program for the refinement of the crystal structure, University of Göttingen, Germany.
- [6] 1992, *International Tables for Crystallography*, edited by A. J. C. Wilson, Vol. C (Dordrecht: Kluwer Academic Publishers).
- [7] GAVEZZOTTI, A., 1983, OPEC, program for organic packing energy calculations, *J. Am. chem. Soc.*, **105**, 5220.
- [8] HORI, K., and OHASHI, Y., 1991, *J. Mater. Chem.*, **1**, 667.
- [9] HORI, K., TAKAMATSU, M., and OHASHI, Y., 1989, *Bull. Chem. Soc. Jpn.*, **62**, 1751.